Level structure of the shell-model nucleus ^{217}At

R.K. Sheline
Chemistry and Physics Departments, Florida State University, Tallahassee, Florida 32306

C.F. Liang and P. Paris
Centre de Spectrométrie Nucléaire et de Spectrométrie de Masse, IN2P3, Centre National de la Recherche Scientifique, Bâtiment 104, 91405 Campus Orsay, France

(Received 25 October 1994)

Alpha recoil separation of a large number of ^{221}Fr sources from a pure almost massless source of ^{225}Ac made possible the study of the level structure of ^{217}At following alpha decay from ^{221}Fr. Alphas in coincidence with all gammas and gammas and electrons in coincidence with ^{221}Fr alphas were used in this study. The levels in ^{217}At can be interpreted in terms of the $\pi(h_{9/2})^3\ \nu(g_{9/2})^{-4}$, $\pi(h_{9/2})^2\ f_{7/2}\ \nu(g_{9/2})^{-4}$, and $\pi(h_{9/2})^2\ i_{13/2}\ \nu(g_{9/2})^{-4}$ shell-model configurations. Considerable similarity in the configurations and energies of the states of ^{217}At and ^{215}At is observed. The only change is in the neutron part of the configurations where the "particle" partial configuration in ^{215}At ($\cdots\nu(g_{9/2})^4$) is replaced by the "hole" partial configuration in ^{217}At ($\cdots\nu(g_{9/2})^{-4}$). No evidence for parity doublets is found in ^{217}At.

PACS number(s): 21.60.Cs, 23.60.+e, 27.80.+w

I. INTRODUCTION

It is important to learn where the border is between nuclei which can best be described by the shell model and nuclei best described by the quadrupole-octupole deformed model. In this regard the level structure of ^{217}At is of considerable interest. With just three protons and six neutrons beyond the double closed shell in ^{208}Pb, ^{217}At might best be described by the shell model. Alternatively, like ^{219}Fr [1] with only two protons more, it might best be described as a reflection-asymmetric nucleus.

In addition, the comparison with the level structure of ^{215}At which has recently been studied [2] should be intriguing. For example, the only shell-model configuration differences between these nuclei should be in the neutron part of the configurations, where ^{215}At would have lowest-lying partial configurations like $\cdots\nu(g_{9/2})^4$, while ^{217}At would have $\cdots\nu(g_{9/2})^{-4}$. These particle-hole relationships in ^{215}At and ^{217}At would be intriguing.

However, although a number of levels have been observed by Leang [3] following alpha decay of ^{221}Fr, only the three lowest have been given tentative [4] or definite [5] spin-parity assignments.

II. EXPERIMENTAL METHODS AND RESULTS

The spectroscopic study of the ^{217}At nucleus is not easily accessible to spectroscopic methods. Thus for example heavy ion reactions without very exotic beams and targets result in too-neutron-deficient At nuclei. Furthermore, nuclear reaction spectroscopy would be very difficult because targets are too far away in mass number. Therefore, we have had to fall back on the alpha decay of short-lived ^{221}Fr as a method of studying the levels of ^{217}At.

A. ^{221}Fr source preparation

A large number of ^{221}Fr ($t_{1/2}$=4.9 min) alpha sources were necessary to obtain satisfactory statistics, particularly for the high energy part of the ^{217}At level structure. Since there is overlap with the alpha spectrum of ^{225}Ac in the low energy region ($E_\alpha < 5830$ keV) of ^{221}Fr, a very careful extraction of ^{225}Ac ($t_{1/2}$=10.0 d) activity from a 3 μCi ^{229}Th source, ^{225}Ra, and other daughter products, was required. For this purpose we used an ion exchange resin and solvents synthesized from ion exchange water followed by vacuum evaporation onto 30 μm Al. This produces an almost massless (< 2 μg/cm^2) ^{225}Ac alpha source. The ^{221}Fr sources were produced by alpha recoil collection on transport tape in vacuum which moves in front of the ^{225}Ac source and transports the ^{221}Fr activity in front of the detectors. In view of the 4.9 min half-life of ^{221}Fr, the transport tape was stationary in front of the ^{225}Ac source for 10 min collecting ^{221}Fr recoils before moving in front of the alpha, gamma, and electron detector system, where it was counted for 10 min while the next ^{221}Fr source was being collected. This process went on automatically for a period of 10 d, producing $\sim$1400 ^{221}Fr sources.

B. Alpha-gamma-electron measurements

The alpha detector used in our measurements was an ion implanted Si wafer 200 mm^2 in area and 100 μm thick

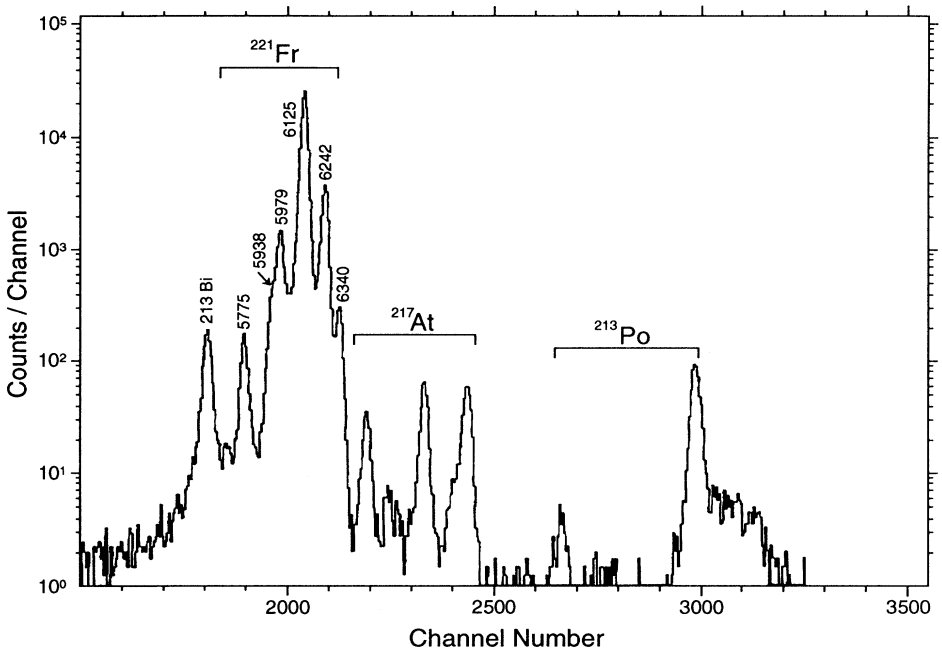

FIG. 1. The alpha spectrum of ^{221}Fr ($t_{1/2}$=4.9 min) and daughters in coincidence with all gammas. Alpha groups from various nuclei are bracketed with the label of that nucleus. Alpha lines from ^{221}Fr are labeled with their energies in keV.

with 16 keV resolution (FWHM). The gamma detector was a 20% efficient coaxial Ge detector with a 0.5 mm Al window. The source was placed between the alpha and gamma detectors in 180° very close geometry. Singles alpha and gamma spectra were taken together with 512 × 2048 channels $\alpha - \gamma$ or $\alpha - e^-$ coincidence measurements. Figure 1 shows the alpha spectrum of ^{221}Fr and its daughters coincident with all gammas, while Fig. 2 presents the gamma spectra in coincidence with all ^{221}Fr alphas. We observed and identified the sum peaks in the gamma coincidence spectra resulting from the large solid angle (~10% of 4π).

Conversion electrons were detected using a Si(Li) wafer 700 mm^2 in area and 6 mm thick (with 2 keV resolution) placed inside an axially increasing magnetic field. This magnetic lens has a large efficiency (2.3%) and a large energy range (10–600 keV) [6]. The conversion electrons are observed at 90° with respect to the alphas on the same side of the ^{225}Ac source. Figure 3, which is a composite of representative results, shows conversion electron spectra in coincidence with the 6242 keV alpha populating the 100.2 keV level in Fig. 3(a), the electron spectra in coincidence with the 6125 keV alpha which populates the 218.0 keV level in Fig. 3(b), and the electron spectra

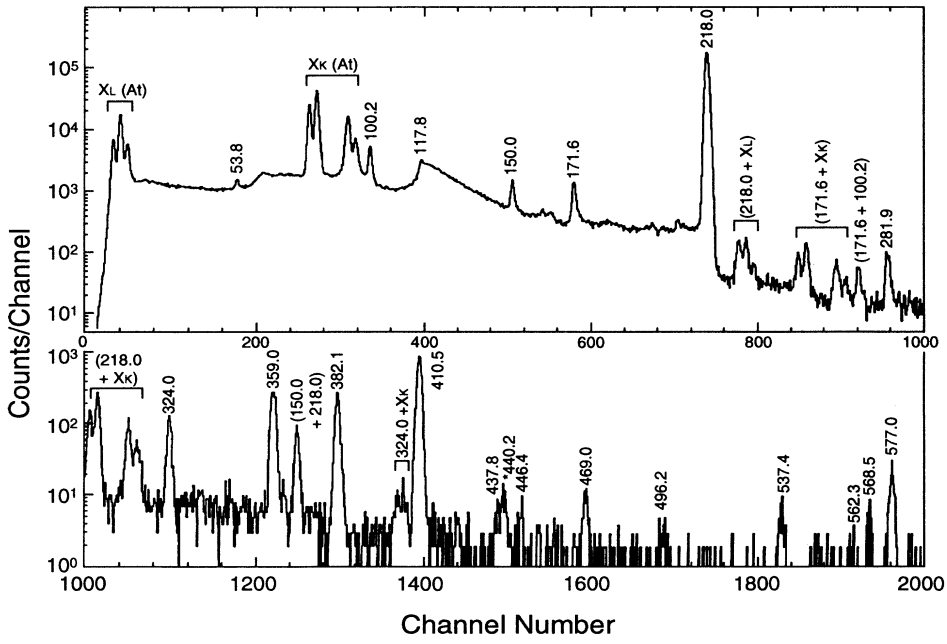

FIG. 2. The gamma spectrum in coincidence with all ^{221}Fr alphas. ^{217}At gammas are labeled with their energies in keV. The 440.2 keV peak marked with an asterisk results from the ^{213}Bi β^- decay.

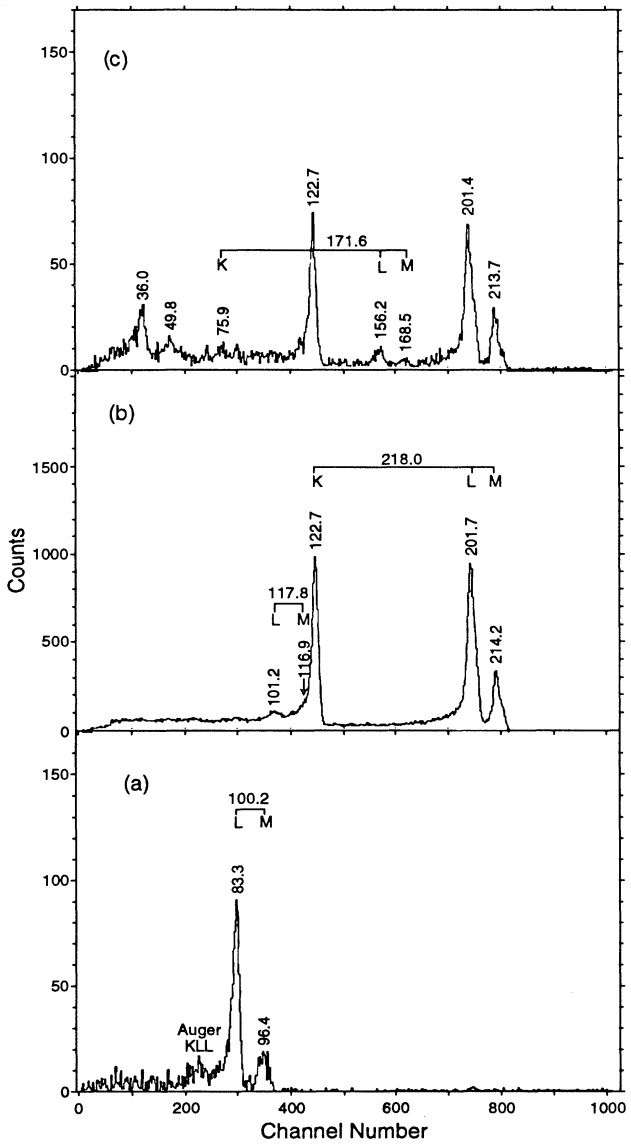

FIG. 3. Conversion electron spectra in coincidence with certain specific alpha lines. (a) The electron spectra in coincidence with the 6242 keV alpha which populates the 100.2 keV level; (b) the electron spectra in coincidence with the 6125 keV alpha populating the 218.0 keV level; (c) the electron spectra in coincidence with the 6075 keV alpha populating the 271.8 keV level. K, L, and M lines are indicated.

in coincidence with the 6075 keV alpha populating the 271.8 keV level in Fig. 3(c). K and L branching ratios and internal conversion coefficients using these data and those of Fig. 2 have made possible the assignment of a number of multipolarities.

The most useful experimental method of constructing the level scheme of ^{217}At is shown in Fig. 4. It represents a sequence of gamma spectra [Figs. 4(a)– 4(d)] in coincidence with groups of ^{221}Fr alpha lines in which the alpha energies are systematically lowered. This in turn implies that we are moving to increasing excitation energies in the ^{217}At level scheme. The gamma spectrum labeled (a) in Fig. 4 corresponds to gammas in coincidence with alphas which populate the 218.0 and 271.8 keV levels; that labeled (b), the 368.1, 382.1, 410.4, and 424.2 keV levels; that labeled (c), the 537.7, 568.8, and 577.0 keV levels; and that labeled (d), the 655 and 664.4 keV levels. These four groups of alphas correspond to the four lowest energy alphas in the ^{217}At spectrum of Fig. 1. The energies in keV of the gamma transitions, x-ray transitions, and in some cases [4(b)] sum lines are indicated in Fig. 4. In this way we move consistently up the level scheme, watching gamma grow in and then decay out with decreasing alpha energy. One automatically places the levels, the transitions which depopulate them, and, by using the conversion electron spectra of Fig. 3, often determines the multipolarities of the transitions.

Table I lists all gamma rays directly observed, together with their energies, intensities, and multipolarities if determined in these experiments. In addition, Table I indicates the assignment of the observed transitions in the level scheme.

III. THE LEVEL SCHEME OF ^{217}At

Using the results of Figs. 1–4 and Table I, the level scheme of ^{217}At is proposed in Fig. 5. It represents >99.7% of the alpha decay of ^{221}Fr. The level structure including the transitions between states has been established with the possible exception of the two very weak transitions of 493 and 562.3 keV, which depopulate the 664.4 keV state.

The spin-parity assignments of the three lowest levels (ground state, 100.2, and 218.0 keV) first suggested in the Table of the Isotopes [4] and recently given "definite" status in Nuclear Data Sheets [5] are confirmed in the present experiment. In addition, the states at 271.8, 368.1, 410.4, and 577.0 keV are assigned spin parities of $3/2^-$, $3/2^-$, $13/2^-$, and $7/2^-$, respectively. The weakest of these assignments is the $3/2^-$ state at 368.1 keV. It decays by an $M1$ and $M1+E2$ into $5/2^-$ and $3/2^-$ states, suggesting spin parity of $3/2^-$ or $5/2^-$. However, since it does not decay to the $7/2^-$ at 100.2 keV with even greater transition energy, the $3/2^-$ spin parity is assigned. Of the other seven states the spin parities of six are listed in parentheses because of uncertainties, and the seventh at 655 keV is given no assignment. All of these states except the 655 and 310 keV states are depopulated by 1–4 transitions, which helps in the tentative assignments. We have assigned the tentative spin parity of $13/2^+$ to the 310 keV level despite the fact that no depopulation of this level is observed because of its similarity to the $13/2^+$ level at 363 keV in ^{215}At. Both of these levels have high α decay hindrance factors (HF's). In ^{215}At a very weak transition was observed between the $13/2^-$ and $13/2^+$ states. We looked for a similar transition in ^{217}At. Unfortunately, its expected energy of 100.4 keV is almost identical with that of the very strong 100.2 keV depopulating the first excited state, and therefore it

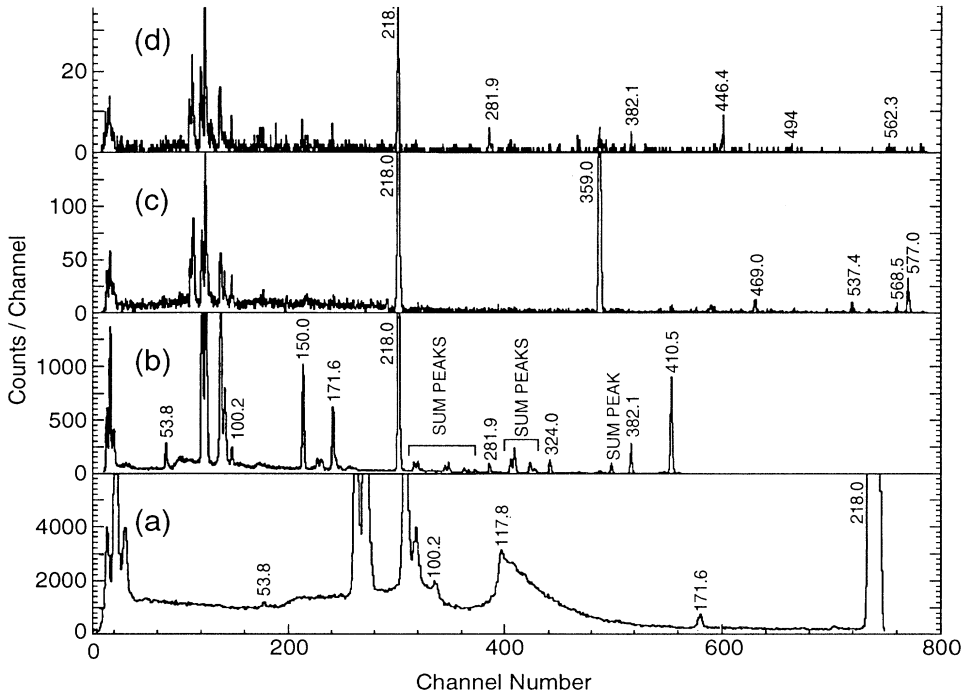

FIG. 4. Gamma spectra in coincidence with groups of ^{221}Fr alpha lines. (a) Gammas observed in coincidence with alphas which populate the 218.0 and 271.8 keV levels; (b) gammas in coincidence with alphas which populate the 368.1, 382.1, 410.4 and 424.2 keV levels; (c) gammas in coincidence with alphas which populate the 537.7, 568.8 and 577.0 keV levels; (d) gammas in coincidence with alphas which populate the 655 and 664.4 keV levels.

is very effectively masked.

One facet of the spin-parity assignments which proved helpful was the consideration of HF's. It should be noted that for ^{217}At they divide into three groupings which are quite separated from each other. The first is from 2.4 to 29, the second from 84 to 180, and the third $\geq$310. A similar grouping of the HF's proved useful in our understanding of ^{215}At. In both cases it appears to be closely related to the predominant configurations. This point will be further discussed below.

The rationale for the level scheme is presented in Fig. 5. It must be noted, however, that although no other spin-

TABLE I. Energies, intensities, multipolarities (when known), and placement in the level scheme of all gammas in ^{217}At following the alpha decay of ^{221}Fr.

$E_\gamma(\Delta E_\gamma)$	$I_\gamma/1000\alpha$	Multipolarity	Level (init.) $\rightarrow$ level (fin.)	α (Expt.)	α (Theor.)
53.8 (0.1)	0.17 (0.05)	$M1$	271.8 $\rightarrow$ 218.0	$\alpha_L = 8 \pm 4$	$\alpha_L(M1) = 11$, $\alpha_L(E2) = 109$
96.3 (0.3)	<0.1	$M1$+$E2$	368.1 $\rightarrow$ 271.8	$\alpha_L > 2.5$	$\alpha_L(M1) = 1.9$, $\alpha_L(E2) = 6.1$
100.2 (0.1)	1.5 (0.2)	$M1$	100.2 $\rightarrow$ 0	$\alpha_L = 1.2 \pm 0.6$	$\alpha_L(M1) = 1.8$, $\alpha_L(E2) = 5.7$
117.8 (0.2)	0.05 (0.02)		218.0 $\rightarrow$ 100.2		
150.0 (0.1)	0.60 (0.10)	$M1$	368.1 $\rightarrow$ 218.0	$\alpha_K = 2.6 \pm 0.5$	$\alpha_K(M1) = 3.1$, $\alpha_K(E2) = 0.3$
171.6 (0.1)	0.66 (0.12)	$E2$	271.8 $\rightarrow$ 100.2	$\alpha_K = 0.3 \pm 0.1$	$\alpha_K(M1) = 2.2$, $\alpha_K(E2) = 0.23$
218.0 (0.1)[a]	113 (10)	$E2$	218.0 $\rightarrow$ 0	$\alpha_K = 0.14$	$\alpha_K(M1) = 1.1$, $\alpha_K(E2) = 0.14$
281.9 (0.3)[b]	0.08 (0.03)		382.1 $\rightarrow$ 100.2 664.4 $\rightarrow$ 382.1		
324.0 (0.2)	0.12 (0.03)	$M1$	424.2 $\rightarrow$ 100.2	$\alpha_K = 0.4 \pm 0.2$	$\alpha_K(M1) = 0.4$, $\alpha_K(E2) = 0.06$
359.0 (0.2)	0.36 (0.10)	$M1$	577.0 $\rightarrow$ 218.0	$\alpha_K = 0.4 \pm 0.1$	$\alpha_K(M1) = 0.3$, $\alpha_K(E2) = 0.05$
382.1 (0.2)	0.31 (0.10)	$M1$	382.1 $\rightarrow$ 0	$\alpha_K = 0.25 \pm 0.10$	$\alpha_K(M1) = 0.24$, $\alpha_K(E2) = 0.04$
410.4 (0.2)	1.1 (0.2)	$E2$	410.4 $\rightarrow$ 0	$\alpha_K = 0.03 \pm 0.01$	$\alpha_K(M1) = 0.20$, $\alpha_K(E2) = 0.035$
437.8 (0.5)	~0.01		537.2 $\rightarrow$ 100.2		
446.3 (0.8)	~0.01		664.4 $\rightarrow$ 218.0		
469.0 (0.5)	0.02 (0.01)		568.4 $\rightarrow$ 100.2		
496.2 (1.0)	~0.01				
537.5 (0.8)	0.02 (0.01)		537.2 $\rightarrow$ 0		
562.3 (1.2)	~0.005		(664.4 $\rightarrow$ 100.2)		
568.4 (1.0)	~0.01		568.4 $\rightarrow$ 0		
577.0 (0.8)	0.04 (0.01)		577.0 $\rightarrow$ 0		
X_K	22.3 (2.0)				

[a]The experimental conversion coefficients were normalized to this 218.0 keV $E2$ transition assuming $\alpha_K = 0.14$.
[b]This 281.9 keV transition was used twice in the level scheme.

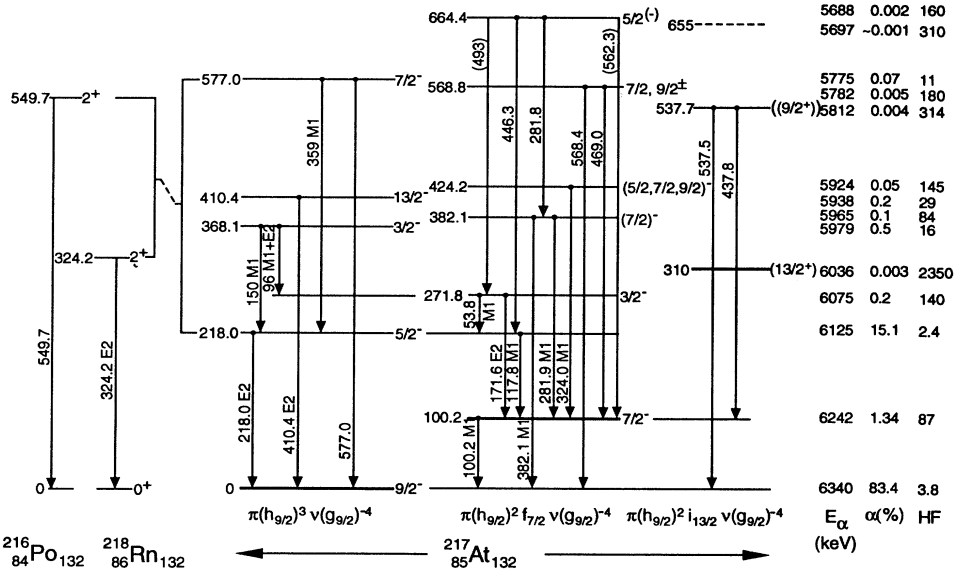

FIG. 5. The level scheme of ^{217}At compared with its isotones ^{216}Po and ^{218}Rn whose partial level schemes are shown to the left. Energies, intensities, and hindrance factors of all alphas populating levels in ^{217}At are shown to the right. Alpha intensity uncertainties are given in Ref. [5]. Energies in keV and multipolarities when known are shown adjacent to transitions.

parity sequence is as satisfactory either experimentally or theoretically as that in Fig. 5, the spin and/or parities listed in parentheses are uncertain. Assuming the correctness of Fig. 5, a number of interesting features of this level scheme are presented in the discussion which follows.

IV. DISCUSSION

A. Shell-model configurations in ^{217}At

We expect to see evidence of the $h_{9/2}$, $f_{7/2}$, and $i_{13/2}$ shell-model states in that order in ^{217}At, similar to ^{215}At [2]. This assumption is based on the level ordering in ^{209}Bi and the theoretical shell model as well as the levels in ^{215}At. These are the groups of states beginning at the ground state, the 100.2 keV state, and the 310 keV state in Fig. 5. The complete configurations are $\{\pi(h_{9/2})^3\nu(g_{9/2})^{-4}\}_{9/2^-}$, $\{\pi(h_{9/2})^2 f_{7/2}\nu(g_{9/2})^{-4}\}_{7/2^-}$, and $\{\pi(h_{9/2})^2 i_{13/2}\nu(g_{9/2})^{-4}\}_{13/2^+}$, as indicated in Fig. 5. The higher energy members of these configurations are then expected at about the energies of the 2^+ states in the isotonic even-even nuclei above the $9/2^-$, $7/2^-$, and $13/2^+$ states. The nuclei ^{216}Po and ^{218}Rn are isotonic to ^{217}At with one less proton and one more proton, respectively. The 2^+ states are observed at 549 and 324 keV, respectively, or at an average energy of 437 keV. This is near but somewhat above the average (393 keV) of the other known states in the $\pi(h_{9/2})^3\nu(g_{9/2})^{-4}$ configuration. However, if the $(2J+1)$ statistical weight factors are taken into account, the average becomes 411 keV, in better agreement with the average of the neighboring even-even nuclei. In a similar way the other members of the $\pi(h_{9/2})^2 f_{7/2}\nu(g_{9/2})^{-4}$ configuration, although less well characterized, lie qualitatively about the same average distance above the $7/2^-$ 100.2 keV state. As noted in the section of this paper on the level scheme it is also of considerable interest that the α decay HF's for populating the three configurations divide into three groups both for ^{217}At and for ^{215}At. By far the lowest HF's (2.4–29) populate the states with configuration $\pi(h_{9/2})^3\nu(g_{9/2})^{-4}$. Because this configuration is strongly populated, a large number of depopulating transitions can be observed, which implies that, as observed, it is the best characterized. The $\pi(h_{9/2})^2 f_{7/2}\nu(g_{9/2})^{-4}$ has intermediate HF's (84–180). Probably this results because of the mixing of these states with the states of the $\pi(h_{9/2})^3\nu(g_{9/2})^{-4}$, since they have the same parity. Finally, the $\pi(h_{9/2})^2 i_{13/2}\nu(g_{9/2})^{-4}$ configuration with opposite parity, so that it cannot mix, has the highest HF's.

B. Comparison between the ^{217}At and ^{215}At level structures

Figure 6 is a comparison of the level structures of ^{217}At and ^{215}At. It is obvious that there is a great similarity. The configurations are identical except that in the neutron part of the configurations the "particle" partial configuration in ^{215}At $(\cdots\nu(g_{9/2})^4)$ is replaced by the "hole" partial configuration in ^{217}At $(\cdots\nu(g_{9/2})^{-4})$. When we consider the level ordering of the $\pi(h_{9/2})^3\ \nu(g_{9/2})^4$ and $\pi(h_{9/2})^3\ \nu(g_{9/2})^{-4}$ configurations, we note that the $3/2^-$ and $7/2^-$ states are interchanged in the two nuclei. However, the ordering of the excited "$f_{7/2}$" and "$i_{13/2}$" configurations is the same in both nuclei with the energies of excitation somewhat lower in ^{217}At. In general, energies of excitation of states in ^{217}At are lower than in ^{215}At. This is probably related to the lower core energies in ^{216}Po and ^{218}Rn (an average of 437 keV) than in ^{214}Po and ^{216}Rn (an average of 537 keV).

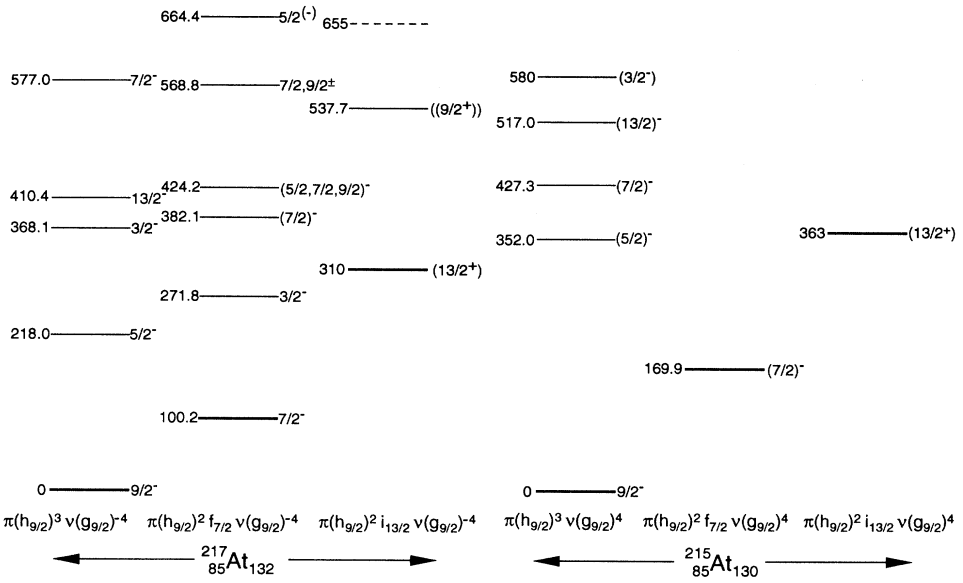

FIG. 6. A comparison of the level structures of ^{217}At (to the left) and ^{215}At (to the right). Note the great similarities in the shell-model configurations and their energies.

C. Relationship of ^{217}At to the quadrupole-octupole deformed model

An alpha decay chain (g.s. → g.s.) from ^{229}Pa to ^{213}Bi is shown in Fig. 7. This chain of nuclei spans the region from the edge of reflection-symmetric nuclei at ^{229}Pa through the quadrupole-octupole deformed region (^{225}Ac and ^{221}Fr) to shell-model nuclei like ^{213}Bi.

It is significant that the HF's are continuously decreasing throughout this sequence. It is not surprising that a very large hindrance factor is observed between ^{229}Pa and ^{225}Ac ground states. The ground states of these nuclei, as indicated in Fig. 7, represent different reflection-asymmetric configurations which would in general not be expected to have large wave function overlap for alpha decay. The much lower HF (8.9) between the ^{225}Ac and ^{221}Fr ground states is at first glance somewhat surprising. It must imply that there is appreciable mixing between the $3/2^{\pm}(0\ -0.3)$ and the $1/2^{\pm}(-1\ -0.5\ -2)$ configurations. Since the ^{221}Fr ground state has the anomalous spin parity $5/2^-$ due to the large decoupling parameter of the $1/2^{\pm}(-1-0.5\ -2)$ configuration it can Coriolis couple with the $5/2^-$ member of the $3/2^{\pm}(0\ -0.3)$ configuration to make the alpha decay more allowed.

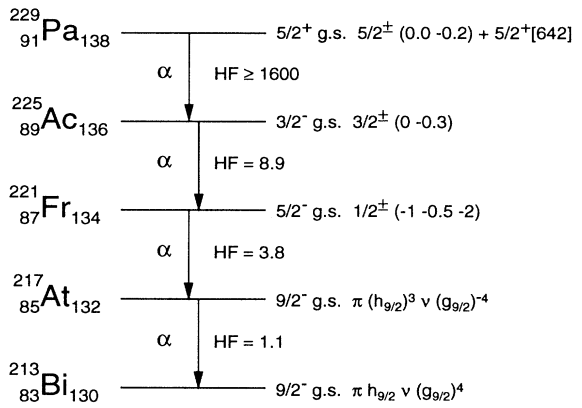

FIG. 7. The alpha decay chain from ^{229}Pa to ^{213}Bi. Only ground state to ground state transitions are shown. The ground state configuration of ^{229}Pa is given as a mixture of the reflection-asymmetric configuration and the Nilsson configuration, whereas the ground state configurations of ^{225}Ac and ^{221}Fr are given in reflection-asymmetric notation only. The ground state configurations of ^{217}At and ^{213}Bi are given in shell-model notation.

Particularly surprising, however, is the HF between the ^{221}Fr and ^{217}At ground states since both different spins and very different configurations are involved. It is clear that the $5/2^-$ ground state of ^{221}Fr is similar to all the members of the $\pi(h_{9/2})^3\ \nu(g_{9/2})^{-4}$ configuration observed, but particularly to the $5/2^-$ and $9/2^-$ states. This probably implies that there is either considerable shell model character in the $5/2^-$ ^{221}Fr ground state or reflection-asymmetric model character in the $9/2^-$ ^{217}At ground state or both.

Finally, the very low HF (1.1) between the ^{217}At and ^{213}Bi ground states is expected since both involve $\pi(h_{9/2})^n$ partial configurations. The entire alpha decay sequence of Fig. 7 is an example of the collapse of quadrupole-octupole deformed Nilsson orbitals into the more degenerate shell-model orbitals.

V. CONCLUSIONS

The level structure of ^{217}At has been studied following the alpha decay of ^{221}Fr. Thirteen levels are assigned definite or tentative spin parities, and one is left unassigned. Alpha decay hindrance factors can be grouped into three sets with values of 2.4–29, 84–180, and >310, which correspond to the population of the configurations $\pi(h_{9/2})^3\ \nu(g_{9/2})^{-4}$, $\pi(h_{9/2})^2\ f_{7/2}\nu(g_{9/2})^{-4}$, and

$\pi(h_{9/2})^2\, i_{13/2}\nu(g_{9/2})^{-4}$.

The level structure of ^{217}At is shown to be very similar to that of ^{215}At with three very similar configurations populated by similar alpha decay hindrance factors. The ^{217}At level energies are systematically lower than those of ^{215}At, which apparently is the result of lower core energies.

The systematics of alpha decay hindrance factors from ^{229}Pa to ^{213}Bi is indicative of the collapse of the quadrupole-octupole Nilsson orbitals into the more degenerate shell-model orbitals.

The low hindrance factors between the $5/2^-$ ^{221}Fr ground state and the $9/2^-$ ground state and the $5/2^-$ 218.0 keV state in ^{217}At (3.8 and 2.4, respectively) imply a similarity between the $5/2^-$ $1/2^{\pm}(-0.1-0.5-2)^{221}$Fr ground state and the $\pi(h_{9/2})^3\ \nu(g_{9/2})^{-4}$ configuration despite the apparent total difference between these two configurations.

ACKNOWLEDGMENTS

One of us (R.K.S.) would like to thank the National Science Foundation for support under Contract No. PHY92-07336 with Florida State University, and the CSNSM and the IPN at Orsay for their hospitality and joint support.

[1] C.F. Liang, P. Paris, J. Kvasil, and R.K. Sheline, Phys. Rev. C **44**, 676 (1991).
[2] C.F. Liang, P. Paris, and R.K. Sheline, Phys. Rev. C **47**, 1801 (1993).
[3] C.F. Leang and G. Bastin-Scoffier, Comp. Rendu Acad. Sc. Paris **226B**, 629 (1968); C.F. Leang, thesis, University of Paris, 1969.
[4] C.M. Lederer and V.S. Shirley, *Table of Isotopes*, 7th ed. (Wiley, New York, 1978).
[5] Y.A. Akovali, Nucl. Data Sheets **63**, 439 (1991).
[6] P. Paris *et al.*, Nucl. Instrum. Methods A (to be published).